Eur. Phys. J. A **31**, 588–592 (2007)
DOI 10.1140/epja/i2006-10268-4

THE EUROPEAN PHYSICAL JOURNAL A

Special Article – QNP 2006

Nucleon form factors and the BLAST experiment

R. Alarcon[a] and the BLAST Collaboration

Department of Physics, Arizona State University, Tempe, AZ 85287, USA

Received: 8 December 2006
Published online: 16 March 2007 –

Abstract. Measurements of the electric and magnetic form factors of the nucleon present a sensitive test of nucleon models and QCD-inspired theories. A precise knowledge of the neutron form factors at low Q^2 is also essential to reduce the systematic errors of parity violation experiments. At the MIT-Bates Linear Accelerator Center, the nucleon form factors have been measured by means of scattering of polarized electrons from vector-polarized hydrogen and deuterium. The experiment used the longitudinally polarized stored electron beam of the MIT-Bates South Hall Ring along with an isotopically pure, highly vector-polarized internal atomic hydrogen and deuterium target provided by an atomic beam source. The measurements have been carried out with the symmetric Bates Large Acceptance Spectrometer Toroid (BLAST) with enhanced neutron detection capability.

PACS. 25.30.-c Lepton-induced reactions – 25.30.Rw Electroproduction reactions – 29.25.-t Particle sources and targets – 29.30.-h Spectrometers and spectroscopic techniques

1 Introduction

The electromagnetic structure of the nucleon is traditionally described in terms of two form factors and it has been extensively studied by the scattering of electrons on nucleons. Experiments on electron-proton scattering have yielded abundant information on the magnetic G_M^p and charge G_E^p form factors of the proton in the range of momentum transfers squared, Q^2, up to about $30\,(\mathrm{GeV}/c)^2$. The information on the neutron form factors comes almost entirely from the scattering of electrons on deuterons or ^{3}He nuclei, and it is much less definite than that on the proton. The difficulty is due mainly to final-state interactions, mesonic currents, and the fact that the form factors of nucleons inside the deuteron or ^{3}He may differ from those of free particles.

Measurements of the nucleon form factors present a sensitive test of nucleon models and QCD-inspired theories. At low momentum transfer, $Q^2 \leq 1\,(\mathrm{GeV}/c)^2$, the pion cloud of the nucleon may play a significant role in the quantitative description of the form factors [1,2], in particular for the electric form factor of the neutron G_E^n in the absence of a net charge. Accurate measurements of the form factors at low Q^2 are required to reduce systematic uncertainty in the extraction of the strange-quark contribution to the nucleon electromagnetic structure as studied in parity violation electron scattering experiments [3].

In recent years the advent of polarized beams, targets, and polarimetry have made possible new classes of experiments aimed at extracting the nucleon form factors utilizing spin degrees of freedom. The general form for the differential cross-section in the exclusive scattering of longitudinally polarized electrons from a polarized target is given by [4]

$$\frac{\mathrm{d}\sigma}{\mathrm{d}e'\mathrm{d}\Omega_e'\mathrm{d}\Omega_N} = \Sigma + h\Delta\,, \tag{1}$$

where h is the helicity of the incident electron, and Σ and Δ are the helicity-sum and helicity-difference cross-sections, respectively. The Σ and Δ cross-sections for the case of elastic scattering from a polarized nucleon can be written as

$$\Sigma = c\left(\rho_L G_E^2 + \rho_T \frac{q^2}{2M^2} G_M^2\right) \tag{2}$$

and

$$\Delta = -c\left(\rho'_{LT}\frac{q}{2^{3/2}M} G_E G_M P_x + \rho'_T \frac{q^2}{2M^2} G_M^2 P_z\right), \tag{3}$$

where c is a kinematical factor, the ρ's are the virtual photon densities, and P_j indicates the polarization of the nucleon along each of the three coordinate axes, of which the z-axis has been chosen parallel to the momentum transfer $\boldsymbol{q}$. The terms containing $G_E G_M$ and G_M^2 can be completely isolated by tuning the target spin polarization. Experimentally one measures spin asymmetries defined as

$$A_{exp} = p_e p_T \frac{\Delta}{\Sigma}\,, \tag{4}$$

[a] e-mail: ralarcon@asu.edu

where p_e and p_T are the electron beam and target polarization, respectively. To separate both terms of the Δ cross-section the target spin is oriented perpendicular (parallel) to the direction of $\boldsymbol{q}$ (*i.e.*, selecting P_x (P_z)).

This work reports preliminary results from new measurements of the nucleon form factors over a range of four-momentum transfer Q^2 between 0.12 and 0.70 $(\mathrm{GeV}/c)^2$ with the BLAST experiment at the MIT-Bates Linear Accelerator Center. The technique makes use of elastic ep scattering of polarized electrons from polarized hydrogen to access the proton form factors, quasi-elastic $(\boldsymbol{e}, e'n)$ scattering from vector-polarized deuterium to get at the charge form factor of the neutron, and inclusive $(\boldsymbol{e}, e')$ scattering from vector-polarized deuterium for the magnetic form factor of the neutron.

2 The BLAST experiment

The BLAST experiment has been designed to measure spin-dependent electron scattering at intermediate energies from polarized targets in the elastic, quasi-elastic and resonance region. Based on the internal-target technique BLAST optimizes the use of a longitudinally polarized electron beam stored in the South Hall Ring of the MIT-Bates Linear Accelerator Center, in combination with an isotopically pure, highly polarized internal target for both hydrogen or deuterium. In case of deuterium the target was both vector and tensor polarized. The polarized target is provided by an Atomic Beam Source (ABS) [5]. The ejected gas molecules are first dissociated into atoms before they pass sections of sextupole magnets and RF transition units to populate the desired single-spin states through Stern-Gerlach beam splitting and induced transitions between hyperfine states (see fig. 1).

This selection process is highly efficient and thus provides nuclear polarizations of more than 70%. The spin state selection was altered every five minutes in a random sequence to minimize systematics. The polarized atoms are injected into a 60 cm long cylindrical target cell with open ends through which the stored electron beam passes. As there are no target windows the experiment is very clean with negligibly small background rates of only a few percent in the prominent channels.

The direction of the target spin can be freely chosen within the horizontal plane using magnetic holding fields. During BLAST data taking, the spin direction pointed at 32° and 47° to the left side of the beam axis in the 2004 and 2005 runs, respectively. At Bates beam currents of up to 225 mA were stored in the ring at 65% polarization and beam lifetimes of 20–30 minutes. The electron beam energy was 850 MeV throughout the BLAST program. The relatively thin target in combination with the high beam intensity yields a luminosity of about $5 \times 10^{31}/(\mathrm{cm}^2\,\mathrm{s})$ at an average current of 175 mA. The Bates storage ring contains a Compton polarimeter to monitor the longitudinal beam polarization in real time and without affecting the beam. The electron spin precession is compensated with a spin rotator (Siberian snake) in the ring section opposite of BLAST. The helicity of the beam was flipped once before every ring fill.

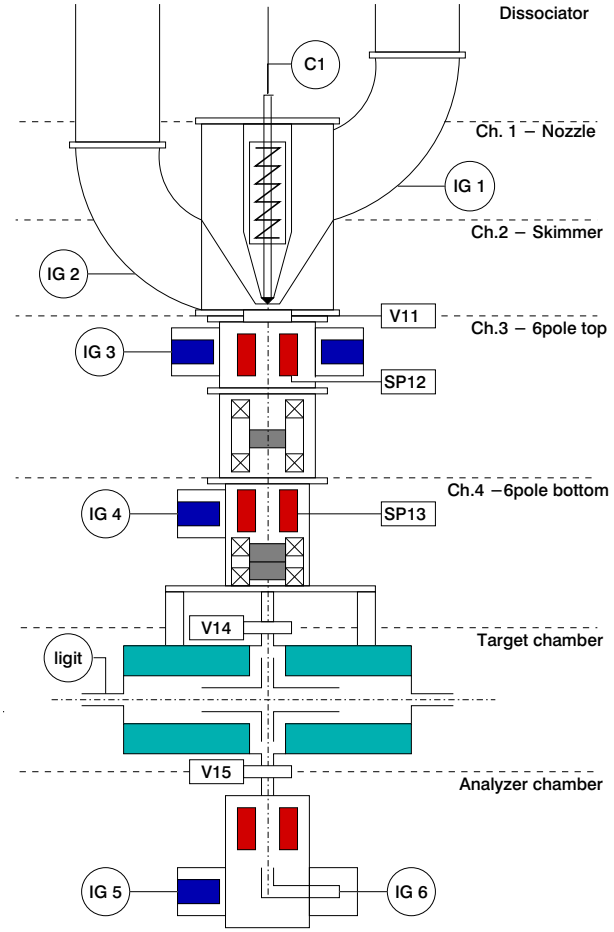

Fig. 1. Schematics of the Atomic Beam Source and the target region. The ABS was embedded in the strong, spatially varying magnetic field of the BLAST toroid [5].

The BLAST detector is schematically shown in fig. 2. It was built as a toroidal spectrometer consisting of eight normal-conducting copper coils producing a maximum field of 3800 G. The two in-plane sectors opposing each other are symmetrically equipped with drift chambers for the reconstruction of charged tracks, aerogel-Cerenkov detectors for e/π discrimination and 1″ thick plastic scintillators for timing, triggering and particle identification. The angular acceptance covers scattering angles between 20° and 80° as well as ±15° out of plane. The symmetric detector core is surrounded by thick large-area walls of plastic scintillators for the detection of neutrons using the time-of-flight method. The thin scintillators in combination with the voluminous wire chambers in front of the neutron detectors were used as a highly efficient veto for charged tracks, making the selection of $(e, e'n)$ events extremely clean. The neutron detectors are enhanced in the right sector with $\approx$ 30% neutron detection efficiency ($\approx$ 10% in the left sector). The reason for this is because

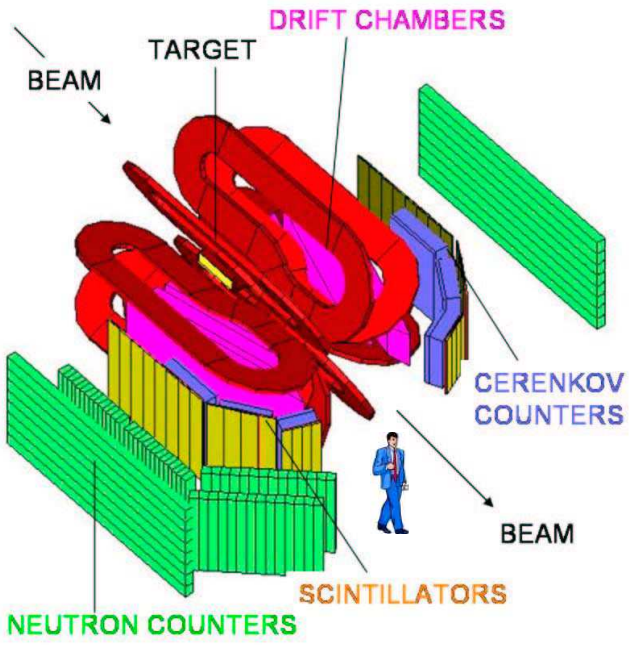

Fig. 2. Schematic, isometric view of the BLAST detector showing the main detector elements.

of the choice of the target spin orientation. The setup allows to simultaneously measure the inclusive and exclusive channels (e, e'), $(e, e'p)$, $(e, e'n)$, $(e, e'd)$ elastic or quasi-elastic, respectively, as well as $(e, e'\pi)$ in the excitation region of the Δ-resonance. By measuring many reaction channels at the same time over a broad range of momentum transfer, the systematic errors are minimal.

3 Results

3.1 Proton electric to magnetic form factor ratio

The polarized hydrogen data were divided into eight Q^2 bins and the yield distributions were in good agreement with results from a Monte Carlo simulation, including all detector efficiencies measured from the data. The BLAST detector configuration is symmetric about the incident electron beam and the target polarization angle is oriented $\sim 45°$ to the left of the beam. Two independent asymmetries of electrons scattered into the beam-left and beam-right sectors, respectively, can be measured simultaneously. The ratio G_E^p/G_M^p can then be determined, independent of p_e and p_T, from the ratio of these experimental asymmetries measured at the same Q^2 value but corresponding to different spin orientations [6].

Preliminary results for G_E^p/G_M^p are shown in fig. 3 with the error bars due to statistical and systematic contributions added in quadrature. Also shown in fig. 3 are published recoil polarization data [7–13], together with a few selected models: a soliton model [14], an extended vector meson dominance model [15], an updated dispersion model [16], a relativistic Constituent-Quark Model

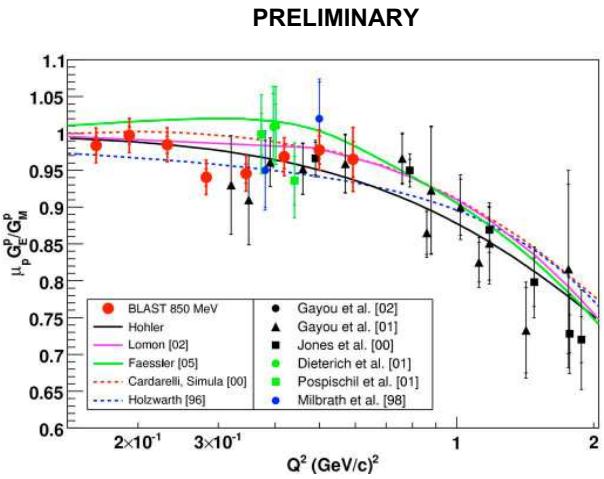

Fig. 3. Preliminary results of $\mu_p G_E^p/G_M^p$ shown with the world polarized data and several models described in the text.

(CQM) with $SU(6)$ symmetry breaking and a constituent-quark form factor [17], and a Lorentz covariant chiral quark model [2]. Using these results and the world differential cross-section data on e-p elastic scattering at the same Q^2 values, the proton electric and magnetic form factors can be extracted and work to this extent is in progress.

3.2 Neutron magnetic form factor

The first experiments to measure G_M^n used electron scattering off unpolarized deuterium in elastic or quasi-elastic kinematics [18–20]. These methods involved significant uncertainties due to the required proton contribution subtraction. Alternatively, the ratio of the cross-sections from the reactions $^2\mathrm{H}(e, e'n)p$ and $^2\mathrm{H}(e, e'p)n$ in quasi-elastic kinematics was used by [21–25]. By measuring the neutron in coincidence, the theoretical uncertainties related to the proton subtraction are eliminated. Furthermore, using the cross-section ratio reduces the dependence of the measurement on nuclear structure. However, these experiments require accurate knowledge of neutron detection efficiency, which is difficult to establish.

Exploiting the recent advances in polarization techniques, the inclusive quasi-elastic reaction $^3\mathbf{He}(\boldsymbol{e}, e')$ has been used for measurements of G_M^n [26–28]. Since in the ground state of $^3\mathbf{He}$ the proton spins anti-align and cancel, the spin of the nucleus is carried by the unpaired neutron [29]. By the simultaneous use of beam and target polarization the experimental asymmetry is related to the ratio of the form factors of the neutron. The systematic uncertainties for these measurements stem mainly from Final-State Interaction (FSI) and reaction mechanism (Meson Exchange Currents (MEC) and Isobar Configurations (IC)) corrections.

With BLAST an alternative measurement of G_M^n has been carried out by using inclusive electron scattering with polarized beam and vector-polarized deuterium target, $^2\mathbf{H}(\boldsymbol{e}, e')$, in quasi-elastic kinematics. The two-body

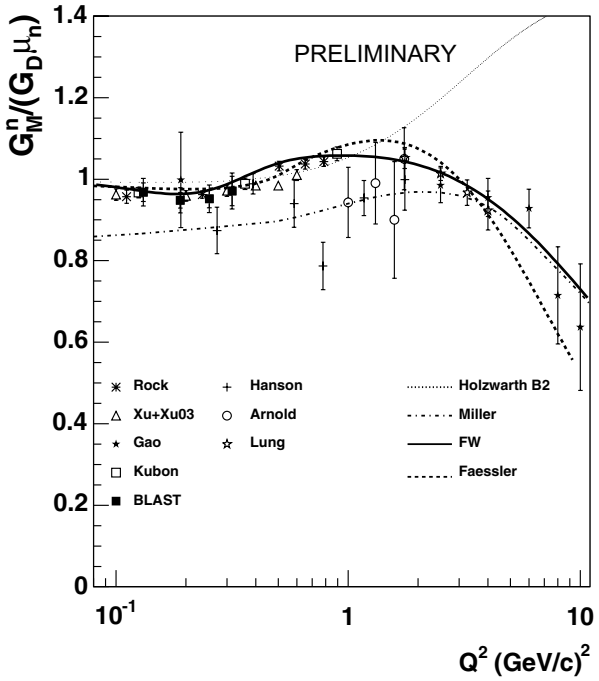

Fig. 4. Sample of the world's data on G_M^n along with the results of the BLAST experiment. The systematic and statistical errors for the BLAST data are added in quadrature. Holzwarth B2 is a soliton model [30], Miller [31] is a cloudy bag model, Faessler [2] is the chiral perturbation theory calculation and FW is the Friedrich and Walcher parametrization [1]. The data are taken from [18–20, 32, 24, 26–28] and the present work.

nature of the deuteron allows analytic solutions to its nuclear structure. Additionally, in the quasi-elastic regime, the FSI, MEC and IC are fairly small. Two data sets were collected, one with target polarization angle of 32° in 2004 (320 kC) and one with 47° in 2005 (550 kC). The asymmetries, the ratio and the sensitivity to G_M^n vary with the target polarization angle. Therefore, the form factor was extracted separately and the results were combined, weighted by their respective error bars. The G_M^n results from this work are shown in fig. 4 along with a selection of the world's data and theoretical calculations.

The systematic uncertainties are dominated by the uncertainty in the target polarization angle which was known to 0.5°. This uncertainty amounted to 5%/degree for the 32° and 3%/degree for the 47° data sets. The second most important uncertainty was due to reconstruction and resolution which amounted to about 1.5%. Radiative effects on the asymmetries in both perpendicular and parallel kinematics were calculated using the MASCARAD software package by approximating the inclusive electrodisintegration channel as an incoherent sum of a proton and a neutron. The uncertainty due to radiative effects associated with this measurement was less than 1%.

The BLAST data agree fairly well with the recent parametrization of [1] and the calculations of [2]. Both of these show a dip in the form factor centered at $Q^2 \approx 0.2\,(\mathrm{GeV}/c)^2$ with a width of $\approx 0.2\,(\mathrm{GeV}/c)^2$.

3.3 Neutron electric form factor

The low-Q^2 region of G_E^n is an ideal testing ground for QCD– and pion-cloud–inspired and other effective nucleon models. Among the four nucleon electromagnetic form factors, G_E^n is experimentally the least known one with uncertainties of typically 15–20%. Significant improvement of the experimental uncertainty is highly desirable and is setting strong constraints for nucleon models. A precise knowledge of G_E^n at low Q^2 is also essential to reduce the systematic errors of parity violation experiments.

With BLAST measurements of G_E^n have been carried out by means of $(e, e'n)$ quasi-elastic scattering using polarized electrons and a vector-polarized deuterium target. The experimental double-spin asymmetry is formed from the measured $(e, e'n)$-yields in each beam-target spin state combination, properly normalized to the collected deadtime-corrected beam charge. For five bins in Q^2, the experimental asymmetry as a function of missing momentum is compared with the full BLAST Monte Carlo result based on deuteron electrodisintegration cross-section calculations by H. Arenhövel [33] with consistent inclusion of reaction mechanism and deuteron structure effects. The electric form factor of the neutron is varied as an input parameter to the Monte Carlo simulation and its measured value is extracted by a χ^2 minimization for each Q^2 bin.

Figure 5 shows the preliminary result for G_E^n from the 2004 run of BLAST along with the world data from polarization experiments [34]. Also shown is the parameterization by Galster *et al.* [35] $G_E^n = 1.91\tau/(1 + 5.6\tau)G_{Dipole}$, where $\tau = Q^2/(4M_n^2)$. The excess of the data over the

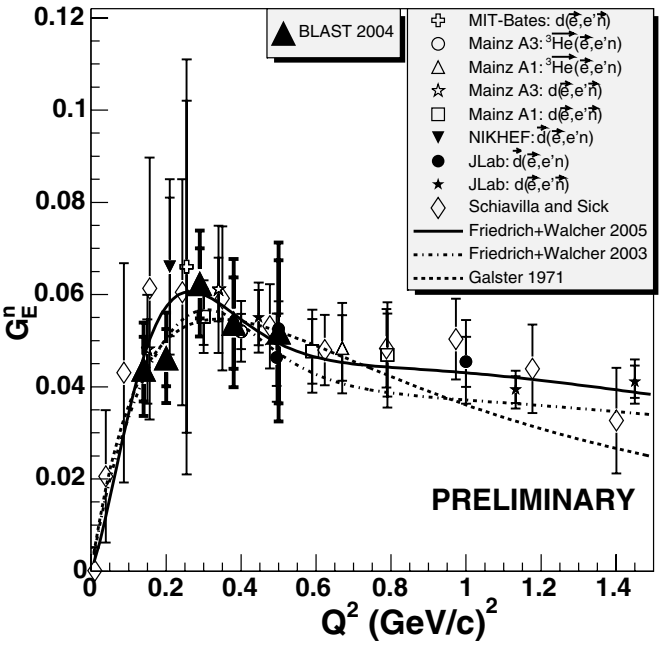

Fig. 5. Electric form factor of the neutron from polarization experiments [34] along with preliminary results from BLAST. The curves are the original parameterization by Galster *et al.* [35] and the recent parameterizations by Friedrich and Walcher [1].

Galster curve at high and at low Q^2 is better accounted for by the more recent parameterization by Friedrich and Walcher [34,1] (FW), who describe all four nucleon form factors as sums of a smooth and a bump part, where the latter is attributed to the role of the pion cloud around the nucleon. The new preliminary BLAST data are quite consistent with both the bulk of existing data as well as with the parameterizations shown in fig. 5, of which the FW parameterization appears slightly favored. Note that the BLAST data is preliminary and based on only about half of the statistics that were acquired in the total run in 2004 and 2005. The preliminary results shown here comprise parts of a PhD Thesis [36] based on the BLAST data taken in 2004. Analysis of the full 2004–2005 data set is in progress [37].

4 Summary

Preliminary results for the electromagnetic form factors of the nucleon have been obtained with the BLAST experiment. The technique utilizes a combination of polarized electron beam, polarized internal gas targets, and a large-acceptance detector. These new measurements cover a range of four-momentum transfer Q^2 between 0.12 and $0.70\,(\mathrm{GeV}/c)^2$. The proton electric to magnetic form factor ratio was measured by elastic ep scattering of polarized electrons from polarized hydrogen. The neutron electric and magnetic form factors were extracted from simultaneous measurements of quasi-elastic $(\boldsymbol{e}, e'n)$ scattering and inclusive $(\boldsymbol{e}, e')$ scattering from vector-polarized deuterium, respectively. The systematic uncertainties are small due to the use of spin degrees of freedom.

References

1. J. Friedrich, T. Walcher, Eur. Phys. J. A **17**, 607 (2003).
2. A. Faessler, Th. Gutsche, V.E. Lyubovitskij, K. Pumsaard, Phys. Rev. D **73**, 114021 (2006).
3. D.S. Armstrong *et al.*, Phys. Rev. Lett. **95**, 092001 (2005).
4. T.W. Donnelly, A.S. Raskin, Ann. Phys. **169**, 247 (1986).
5. D. Cheever *et al.*, Nucl. Instrum. Methods A **556**, 410 (2006); L.D. van Buuren *et al.*, Nucl. Instrum. Methods A **474**, 209 (2001).
6. C.B. Crawford, PhD Thesis, Massachusetts Institute of Technology (2005).
7. M. Jones *et al.*, Phys. Rev. Lett. **84**, 1398 (2000).
8. O. Gayou *et al.*, Phys. Rev. Lett. **88**, 092301 (2002).
9. V. Punjabi *et al.*, Phys. Rev. C **71**, 055202 (2005).
10. O. Gayou *et al.*, Phys. Rev. C **64**, 038202 (2001).
11. S. Dieterich *et al.*, Phys. Lett. B **500**, 47 (2001).
12. T. Pospischil *et al.*, Eur. Phys. J. A **12**, 125 (2001).
13. B. Milbrath *et al.*, Phys. Rev. Lett. **80**, 452 (1998); **82**, 2221 (1999)(E).
14. G. Holzwarth, Z. Phys. A **356**, 339 (1996).
15. E.L. Lomon, Phys. Rev. C **66**, 045501 (2002).
16. H.-W. Hammer, Ulf-G. Meissner, Eur. Phys. J. A **20**, 469 (2004).
17. F. Cardarelli, S. Simula, Phys. Rev. C **62**, 065201 (2000); S. Simula, e-print nucl-th/0105024.
18. S. Rock *et al.*, Phys. Rev. Lett. **49**, 1139 (1982).
19. R.G. Arnold *et al.*, Phys. Rev. Lett. **61**, 806 (1988).
20. A. Lung *et al.*, Phys. Rev. Lett. **70**, 718 (1993).
21. P. Markowitz *et al.*, Phys. Rev. C **48**, R5 (1993).
22. H. Anklin *et al.*, Phys. Lett. B **336**, 313 (1994).
23. E.E.W. Bruins *et al.*, Phys. Rev. Lett. **75**, 21 (1995).
24. G. Kubon *et al.*, Phys. Lett. B **524**, 26 (2002).
25. H. Anklin *et al.*, Phys. Lett. B **428**, 248 (1998).
26. H. Gao *et al.*, Phys. Rev. C **50**, R546 (1994).
27. W. Xu *et al.*, Phys. Rev. Lett. **85**, 2900 (2000).
28. W. Xu *et al.*, Phys. Rev. C **67**, R012201 (2003).
29. J.L. Friar *et al.*, Phys. Rev. C **42**, 2310 (1990).
30. G. Holzwarth, Z. Phys. A **356**, 339 (1996).
31. G.A. Miller, Phys. Rev. C **66**, 032201 (2002).
32. K.M. Hanson *et al.*, Phys. Rev. D **8**, 753 (1973).
33. H. Arenhövel, W. Leidemann, E.L. Tomusiak, Eur. Phys. J. A **23**, 147 (2005).
34. D.I. Glazier *et al.*, Eur. Phys. J. A **24**, 101 (2005) and references therein.
35. S. Galster *et al.*, Nucl. Phys. B **32**, 221 (1971).
36. V. Ziskin, PhD Thesis, Massachusetts Institute of Technology (2005).
37. E. Geis, PhD Thesis, Arizona State University, in preparation.